

## INDIRECT MEASUREMENT OF HERMES III VOLTAGE

T. W. L. Sanford, J. A. Halbleib, J. W. Poukey,  
J. J. Ramirez, J. A. Alexander, G. Douglas,  
R. Mock, and T. Sheridan  
Sandia National Laboratories  
Albuquerque, NM 87185

### Abstract

The peak voltage at the HERMES III diode is measured to be  $19 \pm 2$  MV by three indirect techniques that utilize parapotential flow theory, range of  $H^-$  ions, and radiation output. Associated measurements of peak voltage along the MITL support the measured diode voltage and show that HERMES III operates as a balanced system, with each cavity contributing equally to the power pulse at the diode.

### Introduction

HERMES III is a 14-TW, high-voltage, pulse-power accelerator [1] that drives an electron-beam diode [2] in order to produce an intense burst of  $\gamma$  rays for the study of nuclear radiation effects. Twenty  $\sim 1.1$ -MV,  $\sim 730$ -kA pulses are fed through twenty inductively isolated cavities and added in series by a tapered MITL (magnetically insulated transmission line) adder. An extension MITL delivers this summed output to the diode (Fig. 1).

Of central importance for characterizing the operation of the accelerator, diode, and resulting radiation is knowledge of the peak voltage applied across the diode. In low-voltage, pulse-power accelerators where the peak voltage is less than a few MV, capacitive or resistive voltage dividers can be used to directly measure the voltage. In HERMES III, where the peak voltage is about 20 MV, these direct approaches are difficult, owing to the presence of high electric fields, harsh electron backgrounds, and the long MITL.

In this paper, we describe the measurement of the HERMES III voltage by three indirect methods. These methods [3] have been developed on the HELIA accelerator [4], operating at 3.2 MV and 150 kA. The first method uses measurements of the total and boundary currents in the MITL together with parapotential flow theory [5] to extract the voltage applied across the diode as a function of time. The second

method uses the measurement of the range of  $H^-$  ions [6] accelerated across the AK (anode-cathode) gap of the MITL and provides a lower bound on the peak voltage. The third method uses measurements of the radiation output from the diode together with a computer model of the radiation production [7] and provides an independent check on the absolute scale of the voltage pulse.

### I. Experimental Arrangement

The experimental arrangement is shown in Fig. 1 and is similar to that described in Refs. 1, 2, and 7. Balanced  $B$  loops and current shunts in the anode and cathode of the MITL measure the total and boundary current at the diode and after every fourth cavity along the MITL. Aluminum filters in front of CR-39 film located in the anode measure the range of  $H^-$  ions accelerated across the radial gap of the MITL adjacent to the current monitors. A graphite or optimized Ti/Ta/C target at the anode of the diode is used to convert the energy of the beam electrons to bremsstrahlung radiation. Downstream of the target, an array of 200  $CaF_2:Mn$  TLDs (thermoluminescent dosimeters) measures the time-integrated radiation pattern. Downstream of the array, four collimated CDs (Compton diodes), CD10, CD20, CD30, and CD40, and a SPD (scintillator photo diode) detector measure the radiation versus time at  $10^\circ$ ,  $20^\circ$ ,  $30^\circ$ ,  $40^\circ$ , and  $30^\circ$  from the beam axis, respectively.

### II. Voltage from Parapotential Flow Theory

Parapotential flow theory [5], computer modeling, and comparisons with planar and coaxial magnetic-pressure balance models indicate that the voltage across the MITL or AK gap of the diode can be expressed as an analytic function of the total current, boundary current, and vacuum impedance of the MITL [3]. Figure 2 shows the measured total and boundary current together with the corresponding parapotential voltage at the diode for Shot 483. For 23 shots, the mean and shot-to-shot variation of the voltage is  $20.5 \pm 0.4$  MV at peak power. The absolute uncertainty is  $\pm 10\%$  and is due to the estimated uncertainty in the calibration of the current monitors. Table I shows a comparison of the peak of the parapotential voltage measured at the diode and downstream of cavities 4, 8, 12, 16, and 20 with that expected by scaling the diode voltage (estimated by averaging the diode and MITL range measurements--to be discussed in the next section) by the number of cavities up to the given monitor for Shot 541. Within the uncertainties, the comparison is excellent and gives us confidence in the peak voltage inferred at the diode from flow theory.

Table I. Comparison of voltage obtained from flow theory and  $H^-$  range with that scaled to the given cavity position.

LOCATION	CAVITY 4	CAVITY 8	CAVITY 12	CAVITY 16	CAVITY 20	DIODE
$V_{SCALED}$ (MV)	3.7	7.4	11.2	14.9	18.6	18.6
$V_{H^- RANGE}$ (MV)	$3.6 \pm .2$	$7.4 \pm .2$	$11.0 \pm .3$	$16.0 \pm .4$	$18.5 \pm .4$	$18.2 \pm .4$
$V_{PARAPOTENTIAL}$ (MV)	$3.7 \pm .4$	$6.2 \pm .6$	$11.7 \pm 1.2$	$16.0 \pm 1.6$	$17.9 \pm 1.8$	$18.3 \pm 1.8$

For diode configurations where the radiation field is not sensitive to the time dependence of the electron distribution at the target, the dose-rate scaling relation [8]

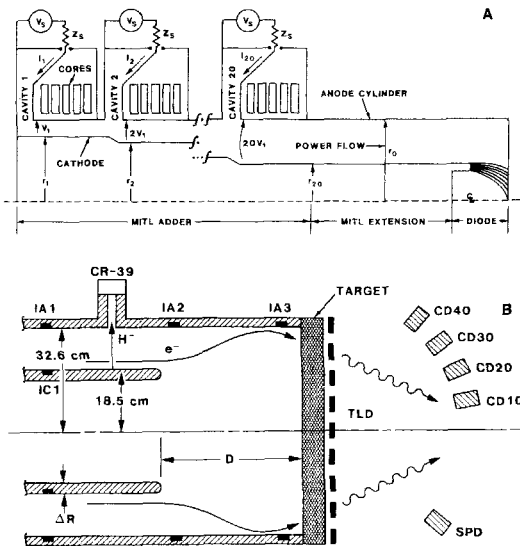


Fig. 1 Schematic of (A) HERMES III Accelerator (B) Diode,  $40 \leq D \leq 100$  cm.

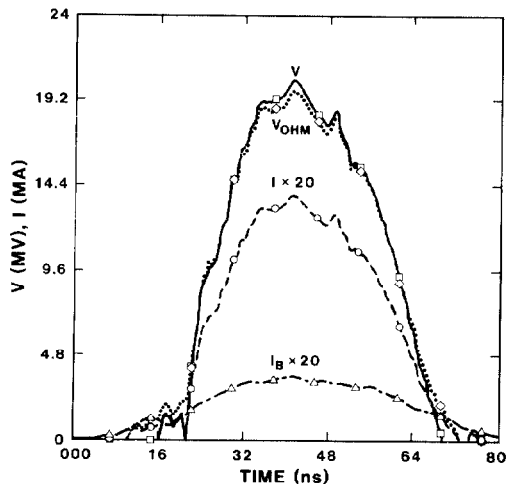


Fig. 2 Measured Total Current,  $I$ , Boundary Current,  $I_B$ , Parapotential Voltage,  $V$ , and  $V_{OHM} = 28.5 I$ .

$$\dot{D}(t) \propto I(t) V(t)^\beta$$

can be used to check the shape of the voltage pulse. For 70-cm AK gaps, we observe experimentally that the FWHM of the radiation pulse varies by typically less than  $\pm 5\%$  over the angular range  $10^\circ$  to  $40^\circ$ , implying little sensitivity to electron dynamics at the target. At the location of CD30 or SPD,  $\beta$  is about 2.2. Accordingly, the scaling relation with  $\beta = 2.2$  should provide a reasonable representation of the radiation pulse measured in CD30 or SPD for our 70-cm AK gap measurements. Data shown in Ref. 2 confirm this expectation and give us confidence that the shape of the measured current and inferred voltage waveforms are correct.

Additionally, near peak power, the parapotential voltage expression reduces approximately to Ohms law. Our steady-state MAGIC computer code [9] simulations [3] indicate little change in impedance with voltage. Thus, the voltage may also be estimated by scaling the measured current using an impedance of  $28.5 \pm .7$  Ohms obtained from our MAGIC calculations. Figure 2 shows that this approximation agrees well with that obtained from flow theory near peak power.

### III. Voltage from $H^-$ Range

Electron emission and bombardment along the cathode of the MITL is sufficient to cause  $H^-$  ions to

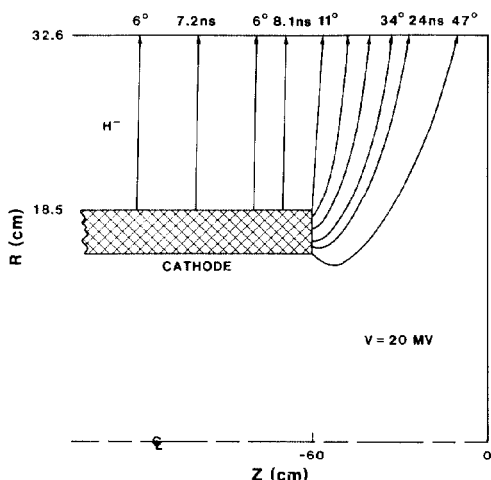


Fig. 3  $H^-$  Ion Trajectories Calculated by MAGIC.

be generated in sufficient numbers early in the power pulse so that measurement of their range can provide an independent bound on the peak voltage. Figure 3 shows typical ion trajectories near the diode calculated using MAGIC. The calculations show that for ions emitted back on the shank 7 to 8 ns are required to transit the radial gap and that their impact angle is about  $6^\circ$  with respect to the anode normal. Experimentally, we observe the voltage pulse (Fig.2) to have a flat top on the order of 10 ns. Thus, measurement of the peak ion range should correspond to the peak diode voltage. Reduced flat top, delayed ion emission, or charge neutralizing reactions of the ion in transit could reduce the maximum KE (kinetic energy) attained so that in principle the range provides only a lower bound on the peak voltage.

We used CR-39 film to detect the ions after the ions have traversed a given thickness of filter. The filter assemblies are made of aluminum foils of well-known thicknesses that varied from  $13 \mu\text{m}$  to  $65 \mu\text{m}$ . The range was determined within one foil thickness by visual inspection of the exposed film. Exposures with filtrations less than the range showed complete saturation ( $> 10^7$  tracks/cm $^2$ ), and exposures with filtrations greater than the range showed few tracks when viewed visually. This lack of tracks was confirmed when a few exposures were scanned by the Sandia Vera track counting system.

The mean and shot-to-shot variation of the diode voltage calculated from the range measurements for 18 shots is  $18.5 \pm 0.6$  MV. Ignoring the possibility of a systematic reduction in voltage mentioned earlier, the absolute uncertainty is estimated to be 8% and is due to uncertainty in the foil thickness, range/energy tables, straggling, and residual energy required for recording with the CR-39 film. Within the uncertainties, the measured peak voltage confirms that obtained from flow theory.

Table I shows a comparison of the voltage obtained from the range measurements at the diode and downstream of cavities 4, 8, 12, 16, and 20 with that expected. As with the comparison of parapotential voltages, this comparison is also in excellent agreement with the scaled values and gives credibility to the peak voltages measured by the range technique. Importantly, the measurements along the MITL indicate that each group of four cavities contribute equally to the voltage measured at the diode. Specifically, the voltages measured at cavities 4, 8, 12, 16, and 20 for four shots indicate that each group of four cavities generates  $3.68 \pm 0.15$  MV. The uncertainty represents shot-to-shot variation. The corresponding contribution each cavity makes to the total voltage is  $0.92 \pm 0.04$  MV.

### IV. Voltage from Radiation Output

Measurement of the radiation downstream of the target provides an independent check on the absolute scale of the voltage waveform and corresponding peak value.

From the measured current and inferred voltage waveforms (shown in Fig. 2, for example), we extract the time-integrated KE (kinetic energy) distribution at the target as illustrated in Fig. 4 for Shot 483. Using this distribution together with a steady-state MAGIC code simulation of the electron flow in the diode for a given AK gap at peak power as input to the electron-photon transport code CYLTRAN [10], we calculate the radiation output.

This MAGIC-CYLTRAN model is described in Ref. 7, where the model is shown to provide a reasonable description of the global features of the time-integrated radiation pattern measured for both graphite and

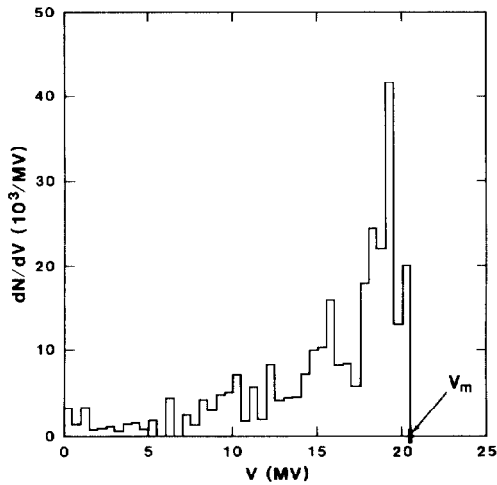


Fig. 4 Electron Kinetic Energy Distribution.

Ti/Ta/C targets over the AK gap range 40 to 100 cm. Our modeling also shows that the integrated dose-area product calculated on the downstream face of the target within a radius of 33 cm is independent of the AK gap over a wide range (Fig. 5). Calculation of the dose-area for a 53-cm AK gap by modeling the time dependence of the radiation using the inferred voltage waveform as input to the model gives the same dose-area within 1.3% as that calculated from our standard model using the steady-state flow pattern generated at peak power. The modeling thus indicates that the measured dose-area provides an excellent measure of the total energy of the beam at the target when compared with our standard model and that the comparison is insensitive to the details of the actual electron flow.

For a given electron KE distribution, the modeling [8] also shows that the dose-area on the target face scales like  $QV^{2.2}$ , where  $Q$  is the total electron charge incident on the target and  $V$  is the peak KE (peak diode voltage). Accordingly, the peak voltage,  $V_m$  (or equivalently the absolute voltage scale), inferred from flow theory can be checked by comparing the calculated dose-area per incident charge,  $(DA/Q)_c$  (calculated using the measured KE distribution having peak KE  $V_m$ ), with the measured dose-area,  $DA_m$ , and the measured incident charge,  $Q_m$ , using the relation

$$V = V_m \left\{ \frac{DA_m}{Q_m} \frac{1}{\left(\frac{DA}{Q}\right)_c} \right\}^{1/2.2}$$

Analysis of 20 shots (half with a graphite and half with a Ti/Ta/C target) over the AK gap range 40 to

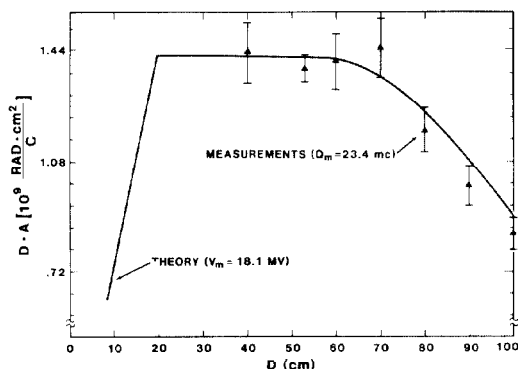


Fig. 5 Measured and Calculated Dose-Area Assuming  $V_m = 18.1$  MV Versus AK Gap for Graphite.

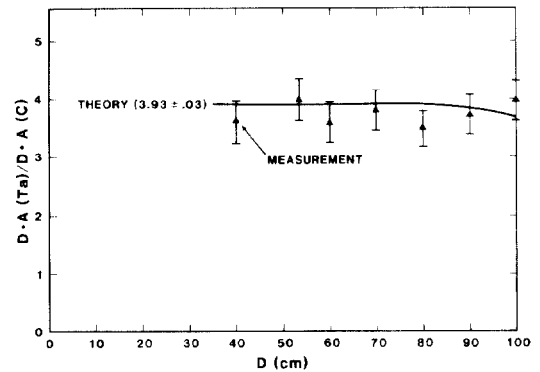


Fig. 6 Ratio of Dose·Area for Ti/Ta/C Target Relative to Dose·Area for Graphite Target.

100 cm gives  $V = 18.1 \pm 0.6$  MV, where the uncertainty represents shot-to-shot variation. The absolute uncertainty is estimated to be  $\pm 9\%$  and is due to uncertainties in the measured charge, uncertainty in the magnitude of the dose-rate saturation in the TLDs (measured by comparing radiochromic film with TLDs), and the calculated dose-area. Within uncertainties, the ratio of the dose-area measured from the Ti/Ta/C relative to that measured from the graphite is consistent with that calculated (Fig. 6). Using only the graphite data, where dose-rate saturation effects are small, we obtain  $V = 18.1 \pm 0.4$  MV. Using only the Ti/Ta/C data, we obtain  $18.0 \pm .7$  MV. As with the range measurements, the peak voltage extracted agrees with that inferred from flow theory within the uncertainty of the analysis.

#### Summary

The peak voltage estimated at the diode using the parapotential flow theory, the range of  $H^-$  ions, and the radiation output are  $20.5 \pm 0.4$  MV,  $18.5 \pm 0.6$  MV, and  $18.1 \pm 0.6$  MV, respectively. The values correspond to the mean and shot-to-shot variation of about 20 shots. The absolute uncertainty is estimated to be about  $\pm 10\%$  for each of the measurements. Within these uncertainties, the measurements are consistent with each other. The peak voltage measured along the MITL corroborate the voltage at the diode and show that HERMES III operates as a balanced system, with each cavity contributing equally to the power flow.

#### References

- [1] J. J. Ramirez et al, in the Proceedings of the 7th International Conference on High-Power Particle Beams, Karlsruhe, Germany, July 4-8, 1988, pp 148-157.
- [2] T. W. L. Sanford et al, *ibid*, pp 326-332.
- [3] T. W. L. Sanford et al, *J. Appl. Phys.* **63**, 681 (1988).
- [4] J. J. Ramirez et al, in the Proceedings of 5th IEEE Pulse Power Conference, pp 143-146.
- [5] J. M. Creedon, *J. Appl. Phys.* **46**, 2946 (1975); **48**, 1070 (1977).
- [6] R. W. Stinnett and T. Stanley, *J. Appl. Phys.* **53**, 3819 (1982).
- [7] T. W. L. Sanford et al, to be submitted to *J. Appl. Phys.*
- [8] T. W. L. Sanford et al, *Nucl. Inst. Meth.*, **B34**, 347 (1988).
- [9] B. Goplen et al, Mission Research Corp. Report No. MCR/WDC-R-068 (1983).
- [10] J. A. Halbleib and T. A. Mehlhorn, *Nucl. Sci. and Eng.* **92** (2), 338 (1986).

This work was supported by the U. S. Department of Energy under Contract DE-AC04-76DP00789.